Stimuli-Responsive Aluminium–Fumarate MOFs from Recycled Aluminium: Phase Evolution, Thermochromism and Gas Sorption

Christophe Adrien Ndamyabera[1]*, Serena Elizabeth Joubert[1] and Henrietta Wakuna Langmi[1]*

[1]*Department of Chemistry, University of Pretoria, Hatfield, South Africa.*

ABSTRACT

Aluminium beverage cans are used as an aluminium-derived metal source for the synthesis of aluminium-fumarate MOF via a hydrothermal reaction, and the resulting MOF is referred to as 1. The synthesized MOF is soaked in methanol, dried, and then activated at 100 °C (1MeOH) and 220 °C (1heat), leading to two different phases identified with the naked eye. The two phases exhibit similar PXRD patterns but slightly different UV-Vis spectra. 1heat is used for the adsorption of water (H_2O) and ammonia (NH_3), where the latter adsorption results in a new phase as confirmed by powder X-ray diffraction (PXRD) and Fourier transform Infrared (FTIR) spectroscopy. Desorption kinetics are investigated using non-isothermal thermogravimetric analysis (TGA). The activation energy for H_2O desorption (Ea = 64.55 kJ/mol) is higher than that for NH_3 (Ea = 54.50 kJ/mol) as expected. Sorption of N_2, CO_2, and H_2 is performed on both 1MeOH and 1heat. For all the gases, 1MeOH shows a higher adsorption capacity than 1heat, which is in corroboration with their respective surface area.

KEYWORDS

waste, recycling, synthesis of MOFs, activation, adsorption

Received: 11 February 2026 Revised: 16 April 2026 Accepted: 19 May 2026

INTRODUCTION

Metal-organic frameworks (MOFs), analogous to other porous solid adsorbents, have been applied for the adsorption or removal of small molecules.[1–3] Their modular nature offers easy functionalization, while their high surface areas, tuneable porosity, and structural diversity enable superior adsorption capacities compared to many conventional porous solids.[4,5] Moreover, they are crystalline materials which allow easy characterization and detailed understanding of host-guest interactions.[5] They can respond to different stimuli such as temperature and guest molecules, which can be monitored by different characterization techniques or even the naked eye.[3,6] MOFs can exhibit a change in color after adsorbing guest molecules, and the interaction between guest molecules and the pore structures in MOFs may sometimes result in a change of the crystal structures, while other MOFs can withstand the same guest molecules as a stimulus.[3,7] Moreover, changes in metal-ligand coordination, ligand to metal charge transfer (LMCT), radical formation in ligand, or framework breathing effect can be characterized.[6,8,9] For example, specific color changes were observed upon application of a range of temperatures in coordination polymers such as Co(II) complex $\{Co(34pbz)_2{\cdot}(H_2O)_4\}_n$ crystals (34pbz is 3-(4-pyridyl)benzoate), where thermal energy alters the coordination environment and electronic structure of the material.[6] Hence, these properties position MOFs as potential candidates for the application in sensing guest molecules and temperature, and for gas storage.

Among MOFs, aluminium-based MOFs are known for their robustness in withstanding harsh conditions such as high temperature, and their moisture tolerance. They stay stable at temperatures of more than 400 °C and show a high capacity to harvest water in arid environments, with the potential of being recycled with high stability.[10] Also, previously reported aluminium-MOFs showed the capacity to adsorb ionic contaminants from aqueous media for the purpose of purification while maintaining structural integrity.[1,10,11] Similarly, MOFs such as Al-BDC, AlBDC-NH_2, Al-BHTA, Al-PMA, and Al-BPDC (with BDC: 1,4-benzenedicarboxylate, BDC-NH_2: 2-aminoterephthalic acid, BHTA: 2,5-dihydroxyterephthalic acid, PMA: 1,2,4,5-benzenetetracarboxylic acid, and BPDC: biphenyl-4,4-dicarboxylic acid), have been reported to effectively remove phosphorous from aqueous solution.[12] These distinguish aluminium-MOFs as the best candidates for various applications. Aluminium is a metal highly used in modern life that is found in food and beverage cans, containers, transportation, and coating materials.[13] As the population and utilisation of technology increase, the use of this metal has become highly demanded. This results in overwhelming waste in the environment, which needs to be addressed. Different technologies have been put in place to recycle aluminium for reusability.[13,14] This includes the use of chemical solutions such as acetic acid, HCl, NaOH, and Na_2CO_3 to generate aluminium salts such as $AlCl_3$, $Al(OH)_3$, and $Al(NO_3)$, useful for the synthesis of MOFs.

The suitability of aluminium MOFs for gas and vapour adsorption, and their robustness, attracts various researchers. In this work, aluminium-fumarate MOF was synthesized using recycled aluminium beverage cans as a source of aluminium and commercially sourced fumaric acid as a ligand. Activation at 100 °C and 220 °C resulted in two different MOF phases, **1MeOH** and **1heat**, respectively. These phases are visually distinguishable by color yet exhibit closely related crystallographic features. The two activated materials were evaluated for the adsorption of N_2, CO_2, and H_2. In addition, the higher temperature phase (**1heat**) was further investigated for the adsorption of ammonia and water to assess whether further color changes might occur. Structural changes induced by guest uptake were examined using PXRD and FTIR spectroscopy, and corresponding desorption kinetics were studied using thermogravimetric analysis.

This study highlights a sustainable approach to MOF synthesis and provides insights into how activation conditions influence MOF properties. By using recycled aluminium cans, it demonstrates the feasibility of successfully producing pure Al-MOFs while probing dependent changes in structure, optical behaviour, and adsorption energetics. Recycled aluminium cans serve as a low-cost precursor, reducing reliance on commercially sourced aluminium salts. This work, therefore, contributes to the development of materials for energy and environmental applications.

EXPERIMENTAL

Materials preparation and sorption study

Aluminium beverage cans from Switch Energy Drink© were washed, followed by the removal of the paint. The cans were sliced into 5 ×

*To whom correspondence should be addressed
Email: U23004462@tuks.co.za and Henrietta.Langmi@up.ac.za

ISSN 1996-840X Online / South African Chemical Institute / http://saci.co.za/journal
© The Author(s) Published under a Creative Commons Attribution 4.0 International Licence (CC BY 4.0)
https://doi.org/10.17159/0379-4350/2026/v80se1a16

5 mm² pieces, and 0.39 g of their weight was soaked in 30 mL of 1 M NaOH and left overnight for dissolution. The solution was filtered and placed in an autoclave containing a solution of 4.84 g of fumaric acid in 30 mL of distilled water. Then 15 mL of acetic acid was added to the mixture, and the sample mixture was placed in an oven and then heated at 90 °C for 90 mins. The oven was set to cool down to room temperature and left overnight. The sample was filtered, and the solids were washed three times with dimethylformamide and then three times with methanol. The as-synthesized material (**1**) was activated as follows: The sample was first soaked in methanol for three days, which involved refreshing with methanol daily. The solid was decanted and dried at room temperature before heating under vacuum at either 100 °C or 220 °C for 24 h to obtain samples **1MeOH** and **1heat**, respectively, as activated MOF materials.

Sorption of H_2O and NH_3 in **1MeOH** and **1heat** was carried out by exposing the solid adsorbents to vapors for 3-5 days. The samples were analysed by TGA at different heating rates (from room temperature to 120 °C) to determine activation energies associated with the removal of guest molecules. Gas sorption (N_2, CO_2, and H_2) for both **1MeOH** and **1heat** was performed using a Micromeritics 3Flex Surface Area Analyzer. A Micromeritics Flowprep was used to prepare samples with masses of 130-140 mg by exposing the samples to a nitrogen flow for 2 h at 60 °C. This was followed by heating of the samples at 120 °C under vacuum for 6 h before sorption analysis. The sorption of CO_2 was conducted at 273 K, while the sorption of H_2 and N_2 was conducted at 77 K. Loading of gas into the samples was performed from 0 to 800 mmHg absolute pressure. The adsorption at maximum pressure was followed by the desorption process.

Characterization

Powder X-ray diffraction (PXRD) patterns were recorded using a Bruker D2 phaser benchtop diffractometer equipped with a Lynxeye detector utilising CuKαradiation (λ = 1.5406 Å). Samples were scanned over a range of 2-theta range of 4–40°. Thermogravimetric analysis (TGA) was carried out using a TA Instrument Q600 SDT instrument. Sample mass of 4–6 mg was placed in open aluminium pans under nitrogen gas flow (50 mL min^{-1}) and heated within the temperature range of 25–500 °C. Fourier Transform Infrared (FTIR) spectra were recorded using a PerkinElmer Spectrum Two FTIR spectrometer equipped with an ATR Diamond crystal accessory for powder materials. The samples were scanned from 400 to 4000 cm^{-1} to analyze functional groups. The absorbance of the samples was analysed using Ultraviolet-visible (UV-Vis) spectrometer. Sample preparation consisted of dissolving the sample in DMF by heating it at 90 °C for 2 h. For all samples, the wavelength was recorded in a range between 200 and 700 nm.

RESULTS AND DISCUSSION

Material activation

Aluminium fumarate MOF (**1**) was successfully synthesized as evident from the PXRD pattern and FTIR spectrum, which show the characteristic diffraction peaks and vibration bands, respectively (Figure 1). The observed diffraction peaks at 12.3, 17.2, 24.3 and 36.9° are similar to those reported for aluminium-fumarate by other research groups and confirm the synthesis of the material with minimal to no impurities.[15,16] This demonstrates that waste aluminium beverage cans can indeed serve as a source of aluminium for the synthesis of this MOF. The crystal structure is reported to be constructed by corner-sharing AlO_6 chains bridged by fumarate linkers with the formula of $Al(OH)(fum)\cdot xH_2O$, (fum = fumarate, x = molecules of water).[16] The as-synthesized material, **1** was white in color and was activated by soaking in methanol followed by heat treatment at 100 °C or 220 °C, to yield two different phases of the MOF denoted as **1MeOH** and **1heat**, respectively, identifiable by the naked eye based on the color difference. The activation processes were repeated for reproducibility and the generation of more materials for further studies. The obtained **1MeOH** remained white while **1heat** exhibited a yellow color as depicted in Figure 2(a). Different characterization techniques were employed to investigate the reason for the color change.

PXRD patterns were used to characterize the two activated phases, and Figure 1(a) indicates that the patterns for **1MeOH** and **1heat** display gentle changes. There is an increase in intensity of the peak at 36.8° relative to the peak at 24.3° for both **1MeOH** and **1heat**, compared to the ones in the pattern for **1**. In addition, they present the emergence of a small peak at 34.7°. This can be attributed to the effect of the removal of guest molecules from the channels. Due to the similarity of the PXRD patterns for both **1MeOH** and **1heat**, it can be suggested that the color change is not due to the effect of structure, contraction of layers or functionality change. TGA plots in Figure S1 show one step before the decomposition of **1** with a weight loss of 34% corresponding to the removal of water and acetic acid guest molecules. The weight loss between 30 and 100 °C of about 3% for **1MeOH** can be attributed to the removal of moisture and methanol. The weight loss between 100 and 300 °C of 7% and 4.3% for **1MeOH** and **1heat**, respectively, is associated with removing very little acetic acid that remained in channels. FTIR spectra in Figure 1(b) show small bands between 3700 and 3740 cm^{-1} in the three

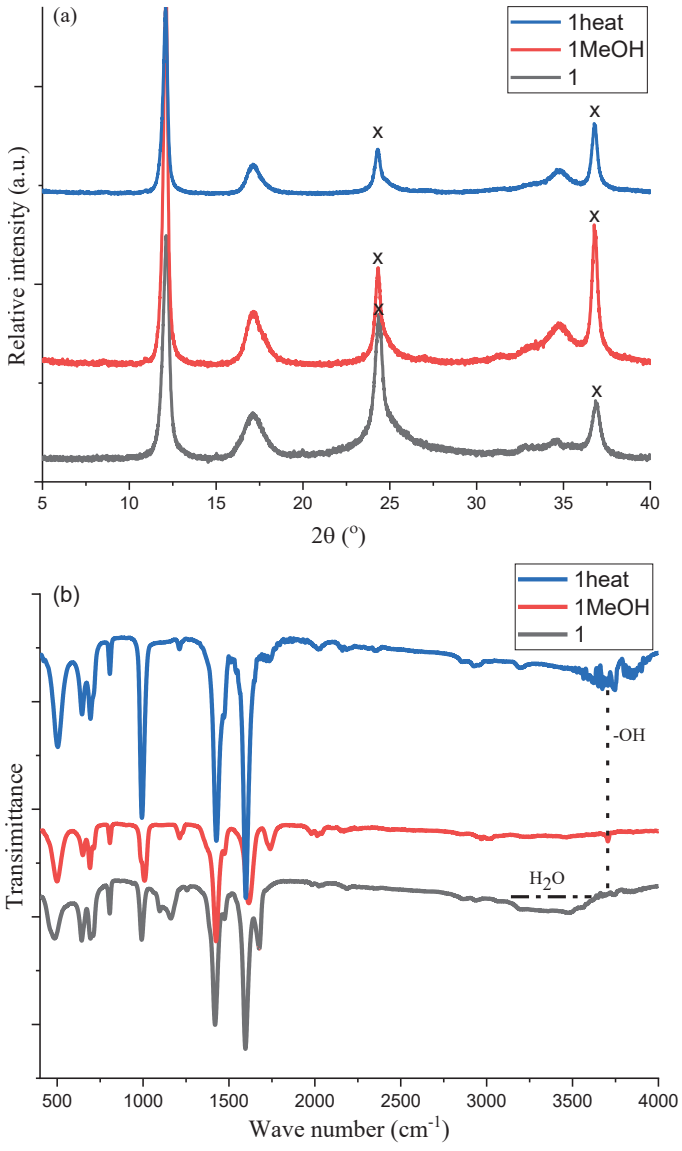


Figure 1: (a) PXRD patterns for **1**, **1MeOH**, and **1heat** and (b) FTIR spectra for **1**, **1MeOH**, and **1heat**.

samples, representing the hydroxyl group. A broad band in a range between 3150 and 3650 cm^{-1} for **1** was attributed to O–H stretching vibrations from water molecules trapped in the channels of the MOF, in agreement with the TGA results. This band is absent from the FTIR spectra for **1MeOH** and **1heat**, indicating that the activation process was effective. However, **1MeOH** spectrum still shows a shoulder band at 1743 cm^{-1}, which can be associated with very little acetic acid that remained in the channels. As the above characterization could not offer information related to the color change, UV-Vis spectroscopy was adopted to analyze possible changes in energy levels.

Figure 2(b) displays the UV spectrum for **1heat** with the absorption band centred at 283 nm, and this is slightly broader than that for **1MeOH,** which is centred at 281 nm. The centre of the absorption band for **1heat** is a little bit shifted by two units to a higher wavelength. The crystal structure is stable, including the hydroxyl groups, at a temperature around 450 °C.[17] It is proposed that the higher activation temperature of 220 °C may cause electron density transfer, which could account for the color change.[18,19] In this case, it is hypothesized that thermochromism arises from thermal excitation of the O → Al LMCT band.[18,20] However, we could not perform more characterization for supporting evidence due to time limitations/limited access to the instruments.

Sorption and kinetic studies

Adsorption of H_2O and NH_3

As the removal of guest molecules at high temperature resulted in a color change, sorption of H_2O and NH_3 vapors was performed on **1heat** to verify if further visual changes might occur. However, the adsorption of water and ammonia vapors led to **1heat@W** and **1heat@NH_3** phases without a color change, Figure 3(a). PXRD patterns in Figure 3(b) for both **1heat** and **1heat@W** are similar. However, there is a slight shift of peaks to the lower 2θ values. Moreover, the intensity of the peak at 36.8° relative to the peak at 24.3° was restored to that in **1**. This suggests supramolecular interactions to some extent between water molecules and the channels of the framework that result in a slight increase in interplanar spacing in the framework. Moreover, the shoulderlike peak at 34.5° in **1heat** disappears in **1heat@W,** and the relative intensity of the peak at 36.8° compared to the peak at 24.3° is reversed and now similar to **1** (see Figure 1a). These confirm a gentle breathing mode in aluminium-fumarate MOF. On the other hand, the pattern for **1heat@NH_3** displays many new peaks such as 22°, 27.8°, 30°, 31.7°, 32.8°, 34°, and 38.4°, indicating a higher reactivity of ammonia compared to water. This shows the changes in structure due to the strong host-guest interactions where ammonia could potentially coordinate to the aluminium centres, and hydrogen bonding with hydroxyl groups.[17] Previous studies of amine adsorption in MOFs had shown that the lone pair of electrons in amines can coordinate to the metal centres.[21] Moreover, the slightly smaller kinetic diameter of NH_3 (2.60 Å) may allow its higher loading compared to H_2O (2.65 Å).

Confirmation of adsorption was further conducted using TGA. Figure 4(a) shows a weight loss of 34.3% at 97 °C for **1heat@W**, attributed to the removal of water, while **1heat@NH_3** has a weight loss of 41 % also at 97 °C, ascribed primarily to the removal of ammonia. These results confirm the successful adsorption of vapors by the

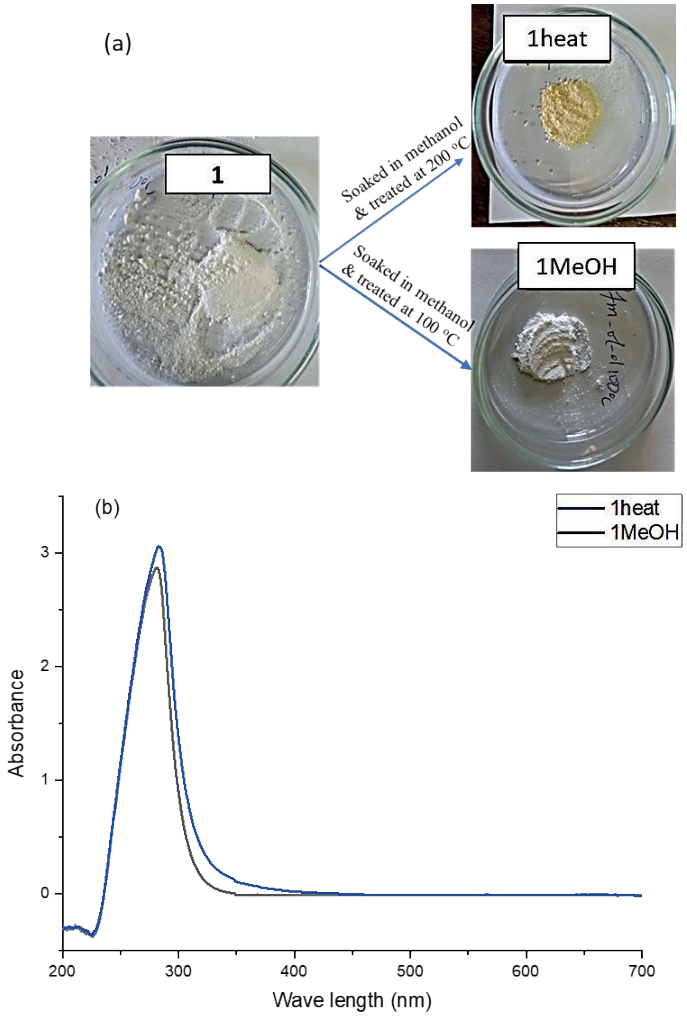


Figure 2: (a) Color change associated with activation temperature and (b) UV-Vis spectra showing the difference in wavelength for **1MeOH** and **1heat**.

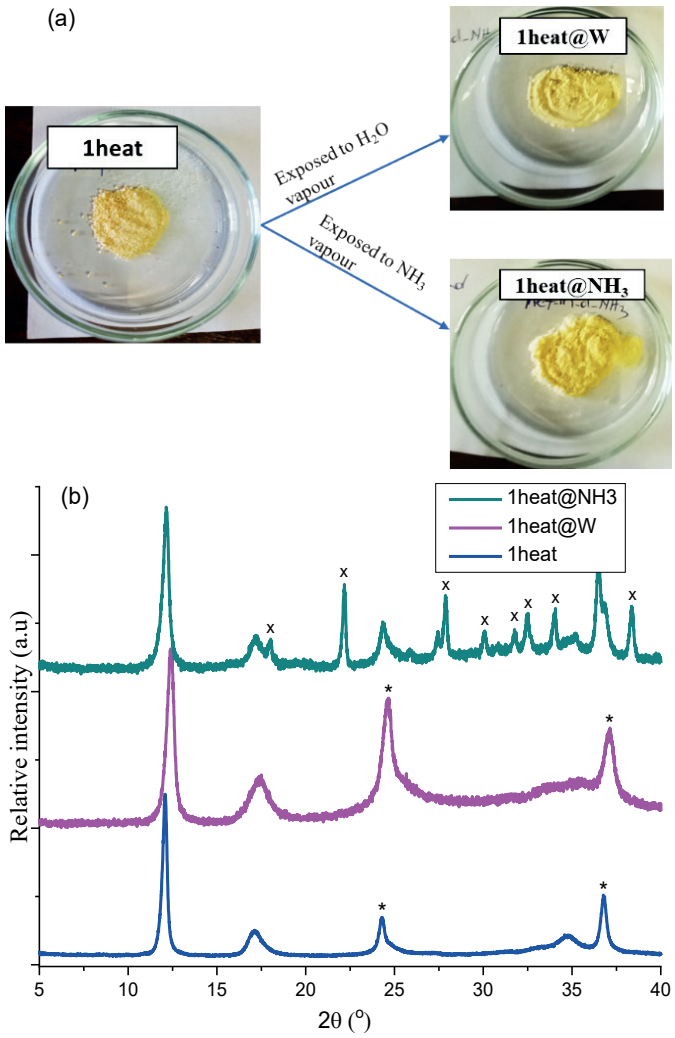


Figure 3: (a) Exposure of **1@heat** to H_2O and NH_3 and (b) PXRD patterns of **1@heat** before and after exposure to H_2O and NH_3.

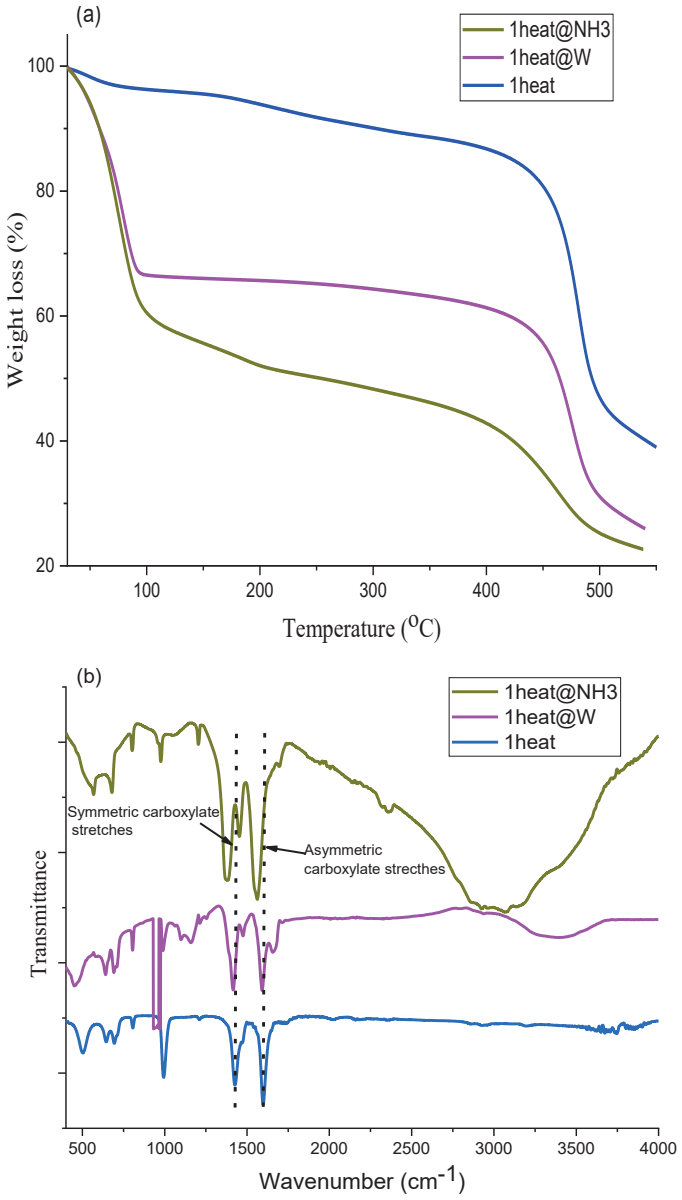


Figure 4: (a) TGA curves showing weight loss for **1heat**, **1heat@W** and **1heat@NH$_3$**, and (b) FTIR spectra for **1heat**, **1heat@W** and **1heat@NH$_3$**.

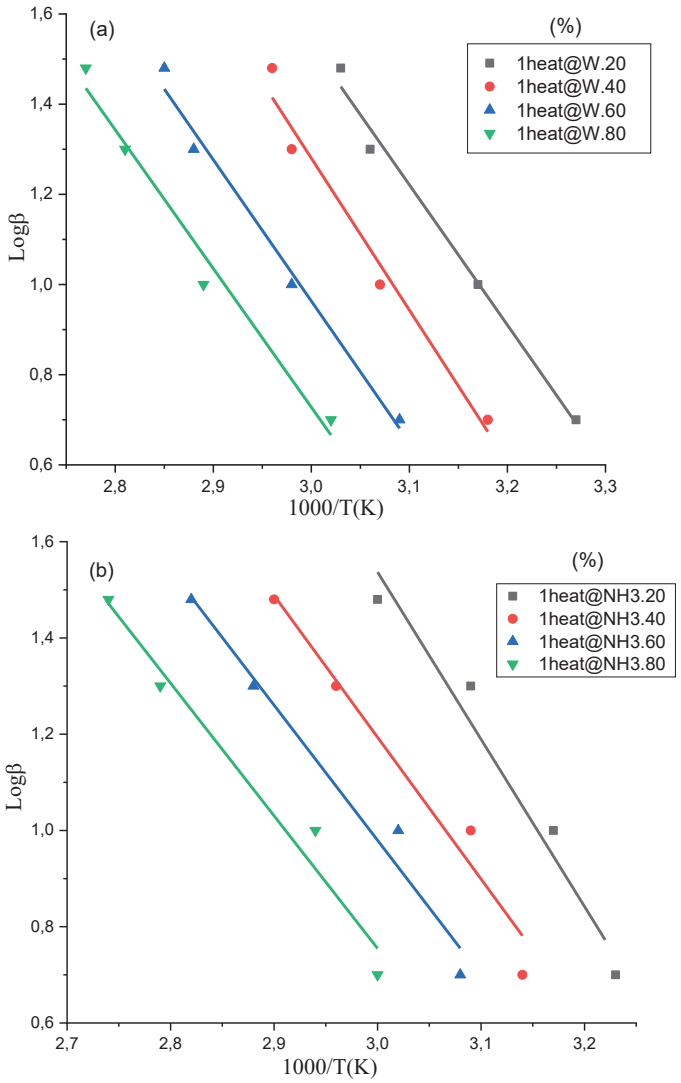


Figure 5: Logarithm of heating rates versus reciprocal absolute temperature of (a)**1heat@W** and (b) **1heat@NH$_3$**.

activated MOFs. Both the **1heat** and **1heat@W** phases decompose at a temperature around 400 °C, similar to **1heat**. It can be seen on the FTIR spectra in Figure 4(b) that both **1heat** and **1heat@W** show asymmetric and symmetric stretching vibrations of carboxylate groups in fumarate at 1598 cm^{-1} and 1425 cm^{-1}, respectively. On the other hand, the asymmetric and symmetric vibrations in **1heat@NH$_3$** are shifted to lower wavenumbers at 1560 and 1375 cm^{-1}, respectively. The shift of the band suggests strong interactions between carboxylates and guest molecules. Moreover, shoulders of both asymmetric and symmetric stretches arise at 1653 and 1474 cm^{-1} for **1heat@W** and at 1450 cm^{-1} for **1heat@NH$_3$**, giving rise to both wider and narrower separations between stretches. This suggests the presence of bidentate and monodentate binding of the carboxylate in the two phases.[6,22] Thus, a structural change in metal coordination supporting the observed PXRD changes.

After adsorption of H_2O and NH_3 in **1heat**, non-isothermal analysis of the solid-state reaction was carried out. Using Ozawa model-free method,[23] TGA was used to determine the activation energy (Ea) associated with the desorption of H_2O and NH_3. The method is based on heating at various heating rates, and for a certain fraction of guest molecules removal, temperatures are recorded. The guest molecules removal is computed as percentages corresponding to the weight loss (α). For each heating rate, the weight loss associated with its corresponding temperature for the removal of guest molecules was used to determine the Ea using the following equation:

$$\log\beta\alpha = \log(A\alpha\, Ea\alpha/g(\alpha)R) - 2.315 - 0.457(Ea\alpha/RT\alpha).$$

where βα is the heating rate, Aα is the frequency factor, Eaα is the activation energy, Tα is the temperature at each weight change to a given fraction, and g(α) refers to the kinetic model. Figure S2(a) for **1heat@W** and S2(b) for **1heat@NH$_3$** show the different heating rates (5, 10, 20, and 30 °C per min) applied to heat a sample mass of between 4 and 5 mg. The removal of guest molecules, expressed as a percentage, is plotted against temperature until complete desorption of the guest molecules.

Using Figure 5(a) and 5(b) for **1heat@W** and **1heat@NH$_3$**, respectively, logβα was plotted against reciprocal absolute temperature (using 1000/T K^{-1} expression), giving a straight line. Each plot corresponds to a fraction of guest molecules removal shown as 20, 40, 60, and 80%. The slope of each trend line that gives the activation energy,[23] was equated to − 0.457(Eaα/RTα) from the above equation to compute the activation energy of desorption corresponding to each conversion level. In this regard, the average Ea calculated for **1heat@NH$_3$** is 54.50 ± 5.18 kJ/mol and for **1heat@W** is 64.55 ± 6.74 kJ/mol. The lower value obtained for **1heat@NH$_3$** might be associated with the lower vapor pressure of ammonia compared to that of water. Both activation energies determined fit in

the expected range, suggesting less energy is needed to remove both guest molecules.

Porosity, and CO_2 and H_2 sorption studies

Both activated forms, **1MeOH** and **1heat** were subjected to N_2 sorption at 77 K for porosity studies. The adsorption isotherms as depicted in Figure 6(a) follow the model of type-I adsorption behavior which is characteristic of microporous solid adsorbents.[24,25] Corresponding surface area of **1MeOH** and **1heat** was 963 m^2/g and 799 m^2/g using the BET method, and 1146 and 989 m^2/g using the Langmuir method. These BET surface areas obtained are in agreement with reported values for aluminium-fumarate MOFs.[15,16,26,27] Table 1 displays comparable BET surface areas and pore sizes of the synthesized aluminium-fumarate MOFs and some reported values in the literature. The reported BET surface area ranges from 792 to 1034 m^2/g. Therefore, recycled aluminium cans offer an alternative source of Al^{3+} ions for the synthesis of aluminium-fumarate MOF with textural properties similar to those synthesized from commercial aluminium salts.

Figure 6(b) shows pore size distributions obtained using the Harvath–Kawazoe (H–K) model. The pore widths were predominantly below 7.00 Å, indicative of ultra-microporosity. The pore size intensity in **1heat** was reduced relative to that of **1MeOH**. This could be due to the effect of temperature of activation, whereby activation at 220 °C resulted in the closing of some micropores to some degree, in line with the lower surface area obtained for this material.

Figure 7(a) details the CO_2 adsorption curves obtained at 273 K at pressures up to 1 bar. The adsorption isotherms correspond again to type-I behaviour with adsorption capacity of 85.45 and 77.52 cm^3/g STP attained for **1MeOH** and **1heat**, respectively. The latter has lower CO_2 adsorption capacity, aligning with its lower surface area.

Table 1: Comparison of BET surface area and pore size of aluminium fumarate MOFs

Aluminium fumarate Nº	BET (m^2/g)	Pore size (Å)	Reference
1	1034	-	[15]
2	925	6	[26]
3	792	7	[27]
4	836	7	[27]
5	1021	-	[16]
1MeOH	963	7	This work
1heat	799	7	This work

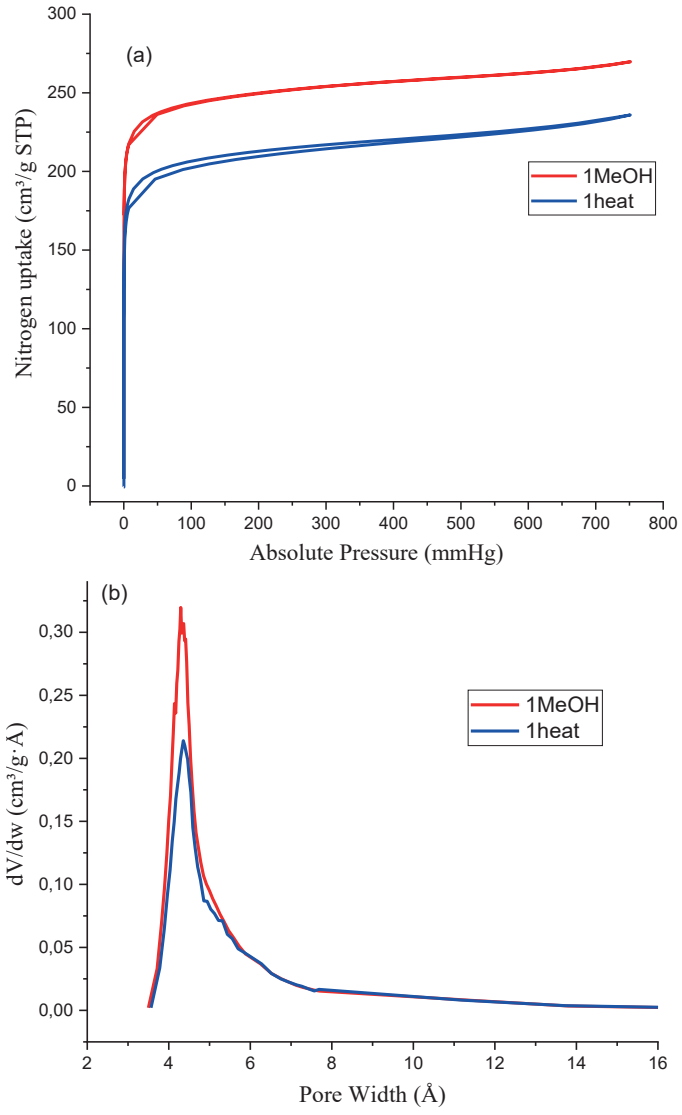


Figure 6: (a) N_2 adsorption/desorption isotherms of **1MeOH** and **1heat**, and (b) Micropore size distribution of **1MeOH** and **1heat**.

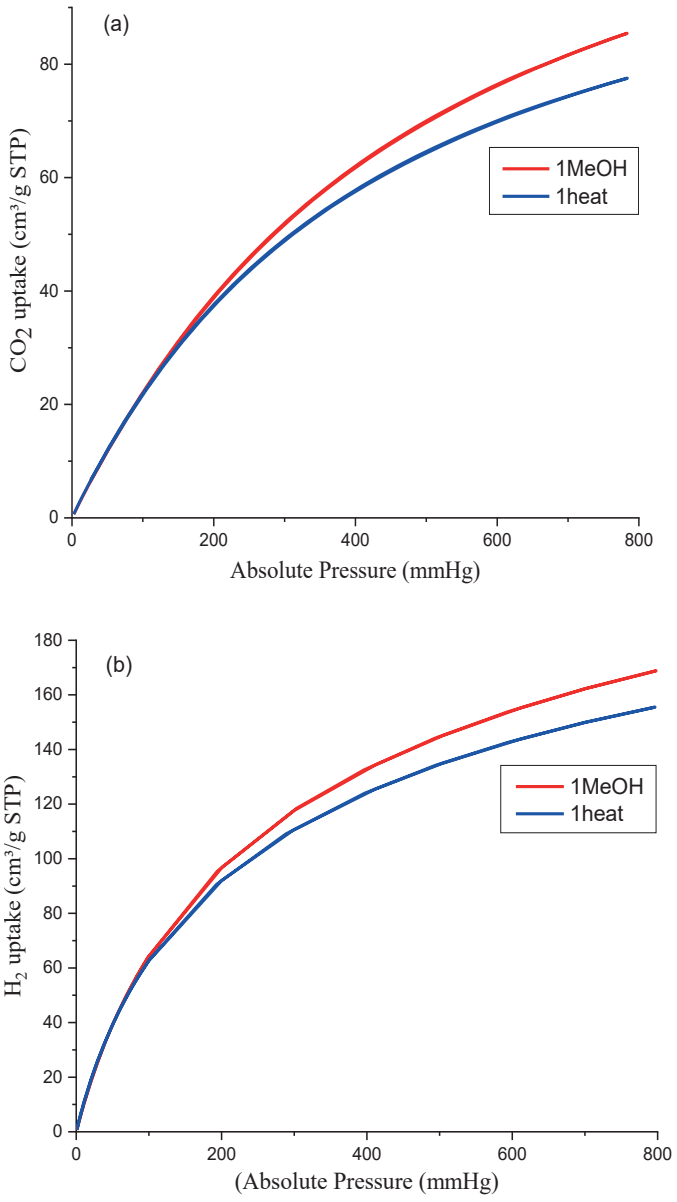


Figure 7: (a) CO_2 adsorption isotherms for **1MeOH** and **1heat**, and (b) H_2 adsorption isotherm for **1MeOH** and **1heat**.

A similar trend of adsorption in Figure 7(b) for H_2 is observed with an appreciable adsorption capacity of 169.4 and 155.5 cm^3/g STP for **1MeOH** and **1heat**, respectively. It can be noted that the adsorption isotherms do not reach a clear plateau, indicating that equilibrium may not have been fully attained under the experimental conditions employed. Therefore, direct comparisons between phases should be interpreted with caution. Additional gas adsorption would be expected if a higher pressure is applied.

CONCLUSION

The synthesis of aluminium-fumarate MOF from recycled aluminium beverage cans was successful. Activation of the MOF at 100 °C resulted in a white product (**1MeOH**) while activation at 220 °C yielded a yellow product (**1heat**), identified as two phases based on the two colors observed with the naked eye. UV-Vis spectra of the activated materials showed slight differences and revealed that the higher activation temperature possibly led to electron density transfer, which may account for the change in color. **1heat** was used for the adsorption of H_2O and NH_3. The latter caused a change in the crystal structure of the adsorbent, with the possibility to coordinate to the metal centres. The activation energies determined for desorption of both H_2O and NH_3 were 54.50 ± 5.18 kJ/mol and 64.55 ± 6.74 kJ/mol, respectively. The BET surface area of **1MeOH** was higher than that of **1heat**, which is attributed to the closure of pores in **1heat** due to the high temperature used during activation. Both phases showed appreciable adsorption for N_2, CO_2 and H_2, with **1MeOH** having a higher adsorption capacity. This work validates the recycling of waste materials as a source of metal centres for the synthesis of MOFs. As aluminium-based MOFs are stable in aqueous media, work on the adsorption of compounds containing nitrogen from water for the purpose of purification is ongoing in our laboratory.

SUPPLEMENTARY INFORMATION

Supplementary information is provided in a separate document.

ACKNOWLEDGEMENTS

Funding from the MAST3RBoost project - Horizon Europe work program funded by the European Union under Grant Agreement No. 101058574 is gratefully acknowledged. The South African Research Chairs Initiative (SARChI) of Department of Science and Innovation and National Research Foundation (NRF, Grant Number: 2090155358), and NRF CPRR (Grant number: 021558637) are also acknowledged.

CREDIT AUTHORSHIP CONTRIBUTION STATEMENT

C. A. N: Conceptualization, methodology, formal analysis, investigation, project administration, validation, and writing – original draft. S. E. J: Investigation and data curation. H W. L: Conceptualization, methodology, funding acquisition, project administration, resources, supervision, validation, and review & editing. All authors have reviewed and approved the final version of the manuscript for publication

CONFLICTS OF INTEREST

There are no conflicts to declare.

DECLARATION OF GENERATIVE AI AND AI-ASSISTED TECHNOLOGIES

This work is entirely original and has not been produced, in whole or in part, using AI tools.

AUTHOR ORCIDS

Christophe A. Ndamyabera: https://orcid.org/0000-0002-2605-319X
Henrietta W. Langmi: https://orcid.org/0000-0002-3299-0059

REFERENCES

1. Bouanga Boudiombo JS, Madden DG, Cusack B, Cronin P, Ryan A. State of the art and prospects of zeolites and metal organic frameworks (MOFs) for nitrogen and phosphorus removal in dairy wastewater. Chemosphere. 2023;329:138531. https://doi.org/10.1016/j.chemosphere.2023.138531
2. Qalyoubi L, Al-Othman A, Al-Asheh S. Recent progress and challenges on adsorptive membranes for the removal of pollutants from wastewater. Part I: Fundamentals and classification of membranes. Case Stud Chem Environ Eng. 2021;3:100086. https://doi.org/10.1016/j.cscee.2021.100086
3. Ndamyabera CA, Zacharias SC, Oliver CL, Bourne SA. Solvatochromism and Selective Sorption of Volatile Organic Solvents in Pyridylbenzoate Metal-Organic Frameworks. Chemistry. 2019;1:111–125. https://doi.org/10.3390/chemistry1010009
4. Jhung SH, Lee JH, Yoon JW, Serre C, Férey G, Chang JS. Microwave synthesis of chromium terephthalate MIL-101 and its benzene sorption ability. Adv Mater. 2007:19:121–124. https://doi.org/10.1002/adma.200601604
5. Farha OK, Eryazici I, Jeong NC, Hauser BG, Wilmer CE, Sarjeant AA, Snurr RQ, Nguyen ST, Yazaydin AÖ, Hupp JT. Metal-organic framework materials with ultrahigh surface areas: Is the sky the limit? J Am Chem Soc. 2012;134:15016–15021. https://doi.org/10.1021/ja3055639
6. Mehlana G, Wilkinson C, Ramon G, Bourne SA. Reversible thermo- and mechanochromic behaviour in a 3D hydrogen bonded discrete complex. Polyhedron. 2015;98:224–229. https://doi.org/10.1016/j.poly.2015.06.016
7. Dzesse TCN, Nfor EN, Bourne SA. Vapor Sorption and Solvatochromism in a Metal-Organic Framework of an Asymmetric Pyridylcarboxylate. Cryst Growth Des. 2018;18:416–423. https://doi.org/10.1021/acs.cgd.7b01417
8. Mehlana G, Bourne SA. Unravelling chromism in metal-organic frameworks. CrystEngComm. 2017;19:4238–4259. https://doi.org/10.1039/C7CE00710H
9. Gong T, Yang X, Fang JJ, Sui Q, Xi FG, Gao EQ. Distinct Chromic and Magnetic Properties of Metal-Organic Frameworks with a Redox Ligand. ACS Appl Mater Interfaces. 2017;9:5503–5512 (2017). https://doi.org/10.1021/acsami.6b15540
10. Hanikel N, Prévot MS, Fathieh F, Kapustin EA, Lyu H, Wang H, Diercks NJ, Glover TG, Yaghi OM. Rapid Cycling and Exceptional Yield in a Metal-Organic Framework Water Harvester. ACS Cent Sci. 2019;5:1699–1706. https://doi.org/10.1021/acscentsci.9b00745
11. Liu R, Chi L, Wang X, Wang Y, Sui Y, Xie T, Arandiyan H. Effective and selective adsorption of phosphate from aqueous solution via trivalent-metals-based amino-MIL-101 MOFs. Chem Eng J. 2019:357:159–168. https://doi.org/10.1016/j.cej.2018.09.122
12. Li S, Zhang Q, Yin C, Chen J, Yang X, Wang S. Tuning microscopic structure of Al-based metal-organic frameworks by changing organic linkers for efficient phosphorus removal. J Clean Prod. 2021;292:125998. https://doi.org/10.1016/j.jclepro.2021.125998
13. Deena H, Khadeeja P, Leena PKF, Lekshmi JS, Sreekumar N. Production of industrial coagulant (Poly Aluminium Chloride) from used beverage cans. J Sci Ind Res. *(India)*. 2019;78,448–453.
14. Rabah MA. Preparation of aluminium-magnesium alloys and some valuable salts from used beverage cans. Waste Manag. 2003;23:173–182. https://doi.org/10.1016/S0956-053X(02)00152-6
15. Rivera-Torrente M, Kroon D, Coulet MV, Marquez C, Nikolopoulos N, Hardian R, Bourrelly S, De Vos D, Whiting GT, Weckhuysen BM. Understanding the Effects of Binders in Gas Sorption and Acidity of Aluminium Fumarate Extrudates. Chem - A Eur J. 2022;28:1–11. https://doi.org/10.1002/chem.202103420
16. Jeremias F, Fröhlich D, Janiak C, Henninger SK. Advancement of sorption-based heat transformation by a metal coating of highly-stable, hydrophilic aluminium fumarate MOF. RSC Adv. 2014;4:24073–24082. https://doi.org/10.1039/C4RA03794D
17. Yang D, Gates BC. Characterization, Structure, and Reactivity of Hydroxyl Groups on Metal-Oxide Cluster Nodes of Metal – Organic Frameworks : Structural Diversity and Keys to Reactivity and Catalysis. Adv Mater. 2024;36:2305611. https://doi.org/10.1002/adma.202305611
18. Kusova OLETV, Shcherbakov OSIAB. Highly reversible photochromism in composite WO 3 / nanocellulose films. Cellulose. 2019;26:9095–9105. https://doi.org/10.1007/s10570-019-02716-2
19. Jiang Z, Duan W, Lin W, Yang L, Wu Z, Wang J, Wang S, Du P, Li Q. Cycloparaphenylene and their radicals anchored to a metal–organic

framework. Mater Today Chem. 2022;25:100973 https://doi.org/10.1016/j.mtchem.2022.100973

20. Bin A, Kayani A, Kuriakose S, Monshipouri M, Khalid FA, Walia S, Sriram S, Bhaskaran M. UV Photochromism in Transition Metal Oxides and Hybrid Materials. Small. 2021;2100621(17):1–31. https://doi.org/10.1002/smll.202100621
21. Reineke TM, Eddaoudi M, Fehr M, Kelley D, Yaghi OM. From condensed lanthanide coordination solids to microporous frameworks having accessible metal sites. J Am Chem Soc. 1999;121(8):1651–1657. https://doi.org/10.1021/ja983577d
22. Deacon GB, Phillips RJ. Relationships between the carbon-oxygen stretching frequencies of carboxylato complexes and the type of carboxylate coordination. Coord Chem Rev. 1980;33:227–250. https://doi.org/10.1016/S0010-8545(00)80455-5
23. Ozawa TA. New Method of Analyzing Thermogravimetric Data. Bull Chem Soc Jpn. 1965;38:1881–1886. https://doi.org/10.1246/bcsj.38.1881
24. Lee SY, Park S-J. Determination of the optimal pore size for improved CO2 adsorption in activated carbon fibers. J. Colloid Interface Sci. 2013;389:230–235. https://doi.org/10.1016/j.jcis.2012.09.018
25. Musyoka NM, Ren J, Langmi HW, North BC, Mathe M, Bessarabov D. Synthesis of rGO/Zr-MOF composite for hydrogen storage application. J Alloys Compd. 2017;724:450–455. https://doi.org/10.1016/j.jallcom.2017.07.040
26. Zhou L, Zhang X, Chen Y. Facile synthesis of Al-fumarate metal–organic framework nano-flakes and their highly selective adsorption of volatile organic compounds. Mater Lett. 2017;197:224–227. https://doi.org/10.1016/j.matlet.2017.01.120
27. Teo HWB, Chakraborty A, Kayal S. Formic acid modulated (fam) aluminium fumarate MOF for improved isotherms and kinetics with water adsorption: Cooling/heat pump applications. Microporous Mesoporous Mater. 2018;272:109–116. https://doi.org/10.1016/j.micromeso.2018.06.016